



ELSEVIER

Journal of Physics and Chemistry of Solids 65 (2004) 1403–1407

JOURNAL OF
PHYSICS AND CHEMISTRY
OF SOLIDS

www.elsevier.com/locate/jpcs

Angle resolved photoemission studies on $\text{Sm}_{2-x}\text{Ce}_x\text{CuO}_4$: remnant Fermi surfaces and coupling to (π, π) scattering

H.S. Jin^a, D.H. Lu^b, N.P. Armitage^c, W.H. Choi^a, B.J. Kim^d, S.-J. Oh^d,
S.H. Moon^e, H. Eisaki^f, C. Kim^{a,*}

^a*Institute of Physics and Applied Physics, Yonsei University, Seoul 120-749, South Korea*

^b*Stanford Synchrotron Radiation Laboratory, Stanford, CA 94309, USA*

^c*Department of Physics, UCLA, Los Angeles, CA 90210, USA*

^d*Department of Physics and Center for Strongly Correlated Material Research, Seoul National University, Seoul 151-742, South Korea*

^e*School of Materials Science and Engineering, Seoul National University, Seoul 151-742, South Korea*

^f*Advanced Industrial Science and Technology, Tsukuba, Ibaraki 305-8568, Japan*

Received 5 July 2003; accepted 22 August 2003

Abstract

We report high-resolution angle-resolved photoelectron spectroscopy studies on electron doped superconductors, $\text{Sm}_{2-x}\text{Ce}_x\text{CuO}_4$ ($x = 0$ and 0.15). The results on the undoped ($x = 0$) samples show Cu–O anti-bonding states with an overall dispersion of about 0.3 eV which is similar to other insulating cases. The low energy dispersive feature quickly loses intensity before it reaches the Fermi energy near the anti-ferromagnetic zone boundary, showing a remnant behavior of the original Fermi surface (FS). In doped cases ($x = 0.15$), FS mapping shows suppressed intensities at the Fermi energy where the FS crosses the anti-ferromagnetic zone boundary. This is similar to what was observed on another electron doped superconductor $\text{Nd}_{1.85}\text{Ce}_{0.15}\text{CuO}_4$ which was ascribed being due to the formation of a high-energy pseudogap assisted by $\mathbf{Q} = (\pi, \pi)$ scattering. Similarities and differences in comparison to other compounds are discussed.

© 2004 Elsevier Ltd. All rights reserved.

PACS: 79.60.Jv; 73.21.Ac; 75.50.Cc

1. Introduction

High temperature superconductivity (HTSC) occurs when Cu–O planes are doped with carriers. Undoped Cu–O planes have one electron per site in their anti-bonding band. Band calculation therefore predicts them to be a metal but the strong Coulomb interaction between the electron in the Cu 3d orbitals makes them a Mott insulator. As carriers are doped into Cu–O planes, they recover metallic properties and become a superconductor. It is therefore imperative to study doping dependent properties of Cu–O planes to understand HTSC. Consequently, there have been extensive studies on the subject (these studies were also partly motivated by the opportunities to explore

the long standing issue regarding the evolution from Mott insulator to a metal).

Among others, understanding the electronic structures is one of the most important steps towards the microscopic theory of HTSC. In that regard, angle resolved photoelectron spectroscopy (ARPES) has been by far the most important technique in the field of electronic structure studies of solids. The HTSC research has not been an exception—researchers have studied HTSC materials from insulators to over-doped superconductors [1]. ARPES studies have found *d*-wave gap [2], pseudo gap [3], and large Fermi surfaces (FS) [4] among others.

ARPES studies on HTSCs, however, have been mostly on so called p-type materials. Cu–O planes can be doped either with electrons (n-type) or holes (p-type). The difference from the semiconductor case is that HTSC compounds can not be both electron- and hole-doped and there exist different ‘parent’ materials for different

* Corresponding author. Tel.: +82-2-2123-2609.

E-mail address: cykim@phy.yonsei.ac.kr (C. Kim).

types of dopings. Structurally, the main difference between n- and p-type superconductors is that the oxygens (or halides) found at the apical site of the CuO_6 octahedral unit in p-type materials are missing in n-type materials (Fig. 1).

While there are ample variety of p-type superconductors, there are only a few variations of n-type materials. This naturally resulted in limited electronic structure studies on n-type materials in a strong contrast to the p-type case. Even though there have been earlier studies [5], systematic high resolution ARPES studies on n-type materials become possible only recently [6,7]. The studies performed so far have been mostly on $\text{Nd}_{2-x}\text{Ce}_x\text{CuO}_4$ systems. As is the case for p-type superconductors, it is important to study various compounds to extract the properties that are universal to Cu–O planes. $\text{Sm}_{2-x}\text{Ce}_x\text{CuO}_4$, an n-type superconductor with the maximum reported T_c value of 18 K [8], provides such opportunities.

In this article, we report synthesis and ARPES studies of single crystalline $\text{Sm}_{2-x}\text{Ce}_x\text{CuO}_4$ samples. The aim of the present work is to study the universal features of the electronic structures of n-type compounds by performing doping dependent ARPES studies and comparing the results with those from other compounds. We synthesized crystals with $x = 0$ and 0.15 and performed systematic ARPES studies. The results show differences as well as similarities when compared to results on other compounds and are discussed accordingly.

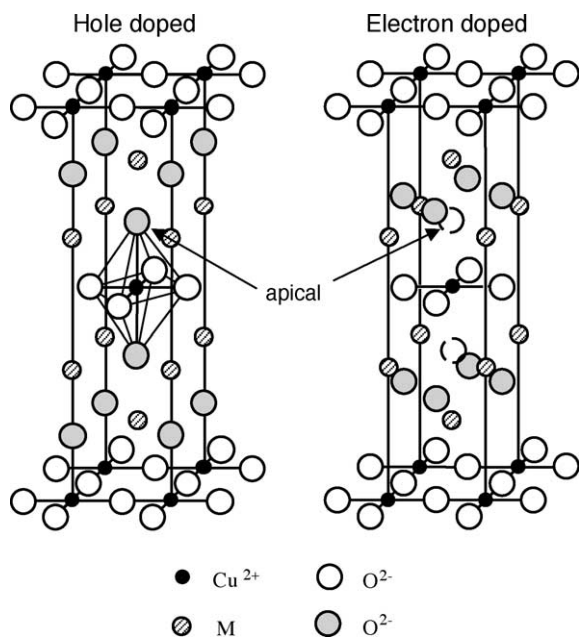


Fig. 1. Crystal structures of typical hole and electron doped superconductors. M represents La or Sr for hole doped compounds and Sm, Nd or Ce in case of electron doped. Atoms at the apical positions of the CuO_6 octahedra are missing in case of electron doped superconductors (dashed circles).

2. Experimental

Single crystals of Sm_2CuO_4 and $\text{Sm}_{1.85}\text{Ce}_{0.15}\text{CuO}_4$ were grown by the flux and travelling-solvent floating-zone methods, respectively. Sm_2CuO_4 crystals (grown by flux method) are platelet shaped with a typical thickness of about 0.5 mm while $\text{Sm}_{1.85}\text{Ce}_{0.15}\text{CuO}_4$ samples have a bar shape of $0.5 \times 0.5 \times 10 \text{ cm}^3$. $\text{Sm}_{1.85}\text{Ce}_{0.15}\text{CuO}_4$ crystals, as $\text{Nd}_{1.85}\text{Ce}_{0.15}\text{CuO}_4$ crystals, become superconducting only when they are reduced. The data reported here were taken on unreduced (non-superconducting) samples. ARPES experiments were performed at beamline 5–4 at the Stanford Synchrotron Radiation Laboratory. For Sm_2CuO_4 , a photon energy of 29 eV was used with 30 meV energy resolution. The temperature was kept at 120 K to prevent charging effects. For $\text{Sm}_{1.85}\text{Ce}_{0.15}\text{CuO}_4$, 16.5 eV light was used with 15 meV energy resolution. Temperature was kept at 10 K during the experiments to make the sample surface last longer. Samples were aligned ex situ by Laue method and cleaved in situ. The cleaved surfaces were flat and shiny, suggesting good surface qualities. The angular resolutions for both cases were about 0.25° . The chamber pressure was kept better than 1×10^{-10} torr during the experiments.

3. Results and discussion

Fig. 2a shows a typical main valence band (VB) spectrum from Sm_2CuO_4 . The feature with the lowest binding energy (marked as σ^*) is thought to be the Zhang-Rice singlet (ZRS) peak which originates from the Cu–O anti-bonding states. The position of the peak is about 0.8 eV from E_F , which is also the case for other insulating compounds such as $\text{Sr}_2\text{CuO}_2\text{Cl}_2$ [10]. In Fig. 2b, we show energy distribution curves (EDCs) along the $(0,0)$ to (π,π) cut. The peak disperses to the higher energy side as the momentum increases from Γ towards (π,π) . Near $(\pi/2,\pi/2)$, the peak's binding energy reaches its minimum value. The peak, in spite of not reaching the Fermi energy, loses the intensity. This is more clearly seen in the density plot of the same EDCs in Fig. 2c. It is clear that the peak disperses about 0.3 eV and then quickly loses intensity near the $(\pi/2,\pi/2)$ point.

Other two dimensional insulating cuprates also show similar dispersion and intensity behavior. The quick drop in the peak intensity across the original FS (which would have existed had there not been strong electron–electron correlations) has especially been discussed in terms of a remnant FS. This can be better seen in a plot of $n(k)$ which is obtained by integrating the spectral weight of the low energy peak. The result is plotted in Fig. 3. It illustrates the steep fall in the intensity across the original FS and is similar to what was observed on another insulating cuprate $\text{Ca}_2\text{CuO}_2\text{Cl}_2$.

It has been a long puzzle how a Mott insulator evolves into a metal upon doping. Does the FS closes out or does it

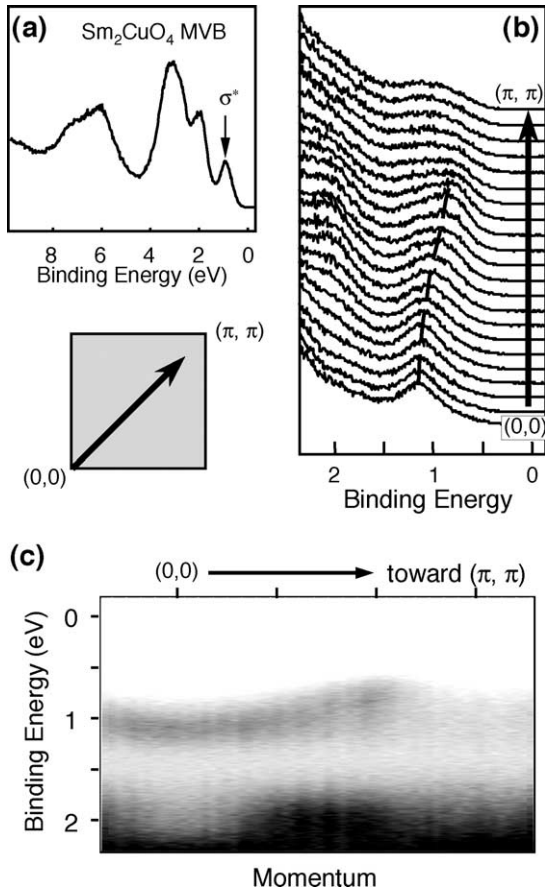


Fig. 2. (a) A typical energy distribution curve for the main VB. This particular one was taken at the Γ point. The peak with the lowest energy is the ZRS peak, originating from the Cu–O anti-bonding state. (b) EDCs of the $(0,0)$ to (π, π) cut around the lowest energy peak. As we go from $(0,0)$ to (π,π) , the peak disperses towards the low energy side and then loses intensity near $(0.5\pi,0.5\pi)$ before it reaches E_F . (c) A density plot of the data in (b). Dispersion and loss of the spectral weight near $(0.5\pi,0.5\pi)$ is more clearly seen. The dotted lines in (b) and (c) are a guide to eyes for the dispersion.

simply disappear? It was initially suggested that the FS closes out near the $(0.5\pi,0.5\pi)$ [10], and then there was indication that the FS simply disappears starting from the $(\pi,0)$ point [11]. A subsequent study on $\text{Ca}_2\text{CuO}_2\text{Cl}_2$ showed that the original FS information is retained even though it is a Mott insulator [12]. The result shown in Fig. 3 also shows that such a remnant behavior occurs in Sm_2CuO_4 .

It is worth note the differences between Sm_2CuO_4 and $\text{Ca}_2\text{CuO}_2\text{Cl}_2$ cases even though they are similar. In case of $\text{Ca}_2\text{CuO}_2\text{Cl}_2$, the $n(k)$ plot shows suppression near the Γ point. A symmetry argument was used to explain this observation by noting that the initial states have $d_{x^2-y^2}$ character (even functions) and thus the photoemission cross section vanishes due to the dipole selection rule [12]. However, this argument is valid only when there is no polarization component of the light perpendicular to the sample surface and thus it alone can not explain the suppression of the weight near Γ . Indeed, Sm_2CuO_4 results

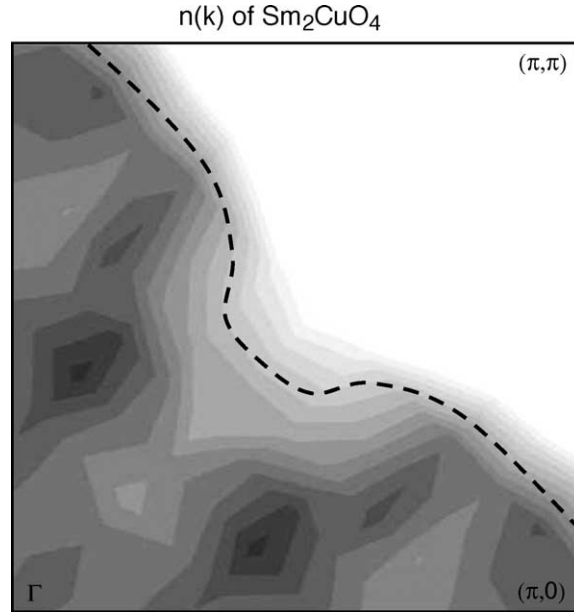


Fig. 3. $n(k)$ plot of the lowest energy peak in a quadrant of the first Brillouin zone. $n(k)$ was obtained by integrating EDCs in a 300 meV energy window around the peak position. We can regard the regions of the BZ where $n(k)$ drops fast as the remnant FS (dotted line).

do not show such suppression near the Γ point even though the low energy states in Sm_2CuO_4 also have $d_{x^2-y^2}$ character. It therefore needs further investigation to resolve this issue.

We now turn our attention to doped cases. Fig. 4 shows EDCs from unreduced $\text{Sm}_{1.85}\text{Ce}_{0.15}\text{CuO}_4$ along the two cuts marked by the two arrows in Fig. 5a. These two cuts are shown for the reason that will be explained later. Panel (a) shows a cut on the Γ to (π,π) line in the first BZ. As we go from Γ towards (π,π) , a peak appears and disperses towards

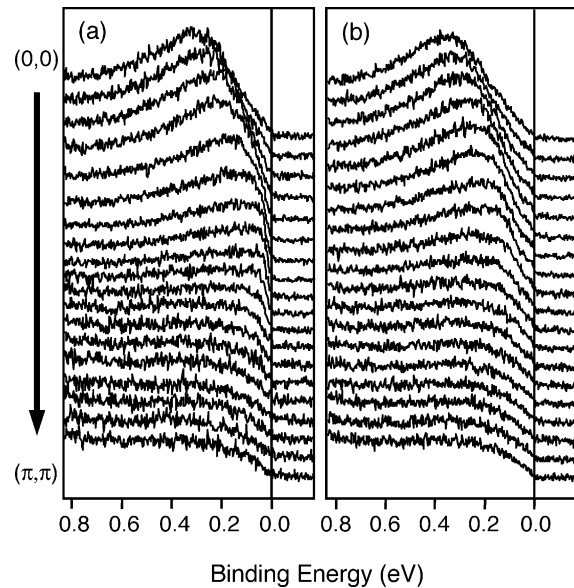


Fig. 4. EDCs along the cuts shown by the two arrows (a and b) in Fig. 5a taken with $h\nu = 16.5$ eV photons.

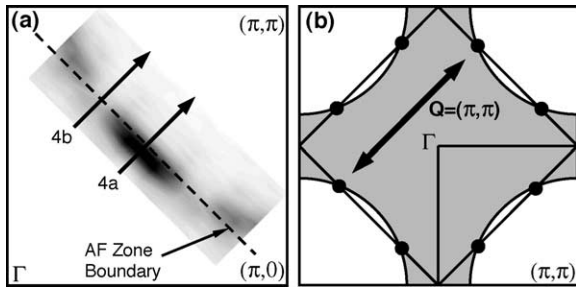


Fig. 5. (a) Plot of the spectral weight at E_F from unreduced $\text{Sm}_{1.85}\text{Ce}_{0.15}\text{CuO}_4$ samples. The high intensity region can be interpreted as the FS. The Dotted line represents the AFZB. The spectral weight is suppressed where FS and AFZB meet. (b) Schematic showing only those regions of FS near the black circles can be coupled with (π, π) scattering.

E_F , sharpens to a sharp peak and then disappears as it crosses the Fermi energy E_F . This behavior of the low energy peak is shared by most of two dimensional cuprates. The situation however is different for the cut shown in panel (b). The peak on this cut disperses towards E_F as the the peak on the Γ to (π, π) cut. Note that the peak loses intensity even though its maximum never comes within 150 meV to E_F in contrast to the data in panel (a). This behavior is similar to what is observed in Sm_2CuO_4 (Fig. 2b) and is also a reminiscence of the high energy pseudo gap found on p-type HTSCs near the $(\pi, 0)$ region [3].

For a better view of the spectral weight at E_F at other regions of the BZ, we show a FS plot in Fig. 5a. What is plotted in the figure is integrated spectral weight about E_F (60 meV integration window). When a peak disperses and reaches the Fermi energy at the FS, the spectral weight at the Fermi energy shows a sharp increase [14]. Therefore, the high intensity region in a circular shape centered at the (π, π) point represents the FS.

The size of the FS is larger than $1/2$ and approximately satisfies the Luttinger volume for $x = 0.15$. In addition, its shape is similar to the calculated results for $\text{Nd}_{1.85}\text{Ce}_{0.15}\text{CuO}_4$ [15]. Even though the size and shape are consistent with the calculated results, it is noted that there are regions of suppressed spectral weight on the FS between $(\pi/2, \pi/2)$ and $(\pi, 0)$ points. The EDCs from these regions (Fig. 4b) show a pseudo-gap behavior as discussed above. A similar pseudo-gap behavior has been observed on $\text{Nd}_{1.85}\text{Ce}_{0.15}\text{CuO}_4$ [9].

A possible way to explain the suppression in the spectral weight is as follows [9]. In solids, coupling of charge carriers to low energy excitations is important, charge density wave being one of the best known examples. If there is a collective mode with a typical momentum $\mathbf{Q} = (\pi, \pi)$ in the system, a phase space argument can show that the suppression would occur in the regions where the FS crosses the antiferromagnetic Brillouin zone (AFBZ) boundary. As depicted in panel (a), the suppressed regions are close to the intersection of the underlying FS and the AFBZ boundary. The schematic in panel (b) shows that the charge carrier which lie at the intersection of the FS and AFBZ boundary

will experience the largest (π, π) scattering since these are the locations that can be connected by the low energy $\mathbf{Q} = (\pi, \pi)$ scattering.

The natural question then is what the low energy collective excitations with a characteristic \mathbf{Q} of (π, π) can be. With the AF phase being stronger and closer to the superconducting phase in electron doped HTSCs, an obvious candidate is the AF fluctuation. It was found in neutron scattering experiments that (π, π) AF fluctuation exists above T_c for both reduced and unreduced crystals [16]. We can not of course rule out other possibilities such as short range fluctuations of the charge density wave, d-density wave or phononic type and there have been theoretical efforts devoted to schemes based on the above general considerations [13,17,18].

Even though the results from $\text{Sm}_{1.85}\text{Ce}_{0.15}\text{CuO}_4$ are similar to those from $\text{Nd}_{1.85}\text{Ce}_{0.15}\text{CuO}_4$, it should be pointed out that the results from $\text{Nd}_{1.85}\text{Ce}_{0.15}\text{CuO}_4$ are on reduced superconducting samples while present results are from unreduced non-superconducting $\text{Sm}_{1.85}\text{Ce}_{0.15}\text{CuO}_4$ crystals. Impurity apical oxygens found on unreduced samples are found to enhance orders in these materials [19]. In addition, there has been a recent report of destruction of the superconductivity with a presence of an AF ordering [20]. In this regards, comparison of data from reduced and unreduced crystals of same compound could shed a light on the issue.

4. Summary

We discussed ARPES results from $\text{Sm}_{2-x}\text{Ce}_x\text{CuO}_4$ ($x = 0$ and 0.15). The data from $x = 0$ show a 0.3 eV dispersion of the low energy peak as is observed in other insulating cuprates. The peak loses its intensity before it reaches the Fermi energy as if there is a ghost Fermi energy. The regions in the k -space where the peak loses intensity are similar to what would have been a FS had there not been strong electron–electron correlation. This behavior is similar to what was found on another insulating cuprate $\text{Ca}_2\text{CuO}_2\text{Cl}_2$ and is viewed as remnant of the underlying FS.

The FS of $\text{Sm}_{1.85}\text{Ce}_{0.15}\text{CuO}_4$ forms an arc centered at the (π, π) point with suppressed regions of spectral weight. The suppression of the spectral weight at the Fermi energy can be understood as opening of pseudo-gaps assisted by low energy $\mathbf{Q} = (\pi, \pi)$ excitations. Future experiments and comparison of the results on reduced and unreduced samples can enhance the understanding of such phenomena.

Acknowledgements

This work is supported by the Korean Science and Engineering Foundation (KOSEF) through the Center for Strongly Correlated Materials Research (CSCMR) at Seoul

National University (2000). SSRL is operated by the DOE Office of Basic Energy Sciences, Divisions of Chemical Sciences and Materials Sciences.

References

- [1] A. Damascelli, Z. Hussein, Z.-X. Shen, *Rev. Mod. Phys.* 75 (2003) 473.
- [2] Z.-X. Shen, et al., *Phys. Rev. Lett.* 70 (1993) 1553.
- [3] D. Marshall, et al., *Phys. Rev. Lett.* 76 (1996) 4841.
- [4] D. Dessau, et al., *Phys. Rev. Lett.* 71 (1993) 2781.
- [5] (a) D. King, et al., *Phys. Rev. Lett.* 70 (1993) 3159. (b) R.O. Anderson, et al., *Phys. Rev. Lett.* 70 (1993) 3163.
- [6] (a) N.P. Armitage, et al., *Phys. Rev. Lett.* 86 (2001) 1126. (b) N.P. Armitage, et al., *Phys. Rev. Lett.* 88 (2002) 257001.
- [7] T. Sato, T. Kamiyama, T. Takahashi, K. Kurahashi, K. Yamada, *Science* 291 (2001) 1517.
- [8] B.K. Cho, J.H. Kim, Y.J. Kim, O. Beom-hoan, J.S. Kimand, G.R. Stewart, *Phys. Rev. B* 63 (2001) 214504.
- [9] N.P. Armitage, et al., *Phys. Rev. Lett.* 87 (2001) 147003.
- [10] B.O. Wells, et al., *Phys. Rev. Lett.* 74 (1995) 964.
- [11] H. Ding, et al., *Phys. Rev. Lett.* 78 (1997) 2628.
- [12] F. Ronning, et al., *Science* 282 (1998) 2067.
- [13] (a) D. Pines, *Z. Phys. B* 103 (1997) 129. (b) J. Schmalian, D. Pines, B. Stojkovic, *Phys. Rev. Lett.* 80 (1998) 3839. (c) A. Kampf, J.R. Schrieffer, *Phys. Rev. B* 42 (1990) 7967.
- [14] This technique became feasible with the advances in the electron spectroscopy techniques and is commonly used in electronic structure studies of layered materials by ARPES. For example, see D.L. Feng, et al., *Phys. Rev. Lett.* 86 (2001) 5550.
- [15] S. Massida, N. Hamada, J. Yu, A. Freeman, *Physica (Amsterdam)* 157C (1989) 571.
- [16] K. Yamada, Y. Kurahashi, R.J. Endoh, G. Birgeneau, *J. Phys. Chem. Solids* 60 (1999) 1025.
- [17] R. Hlubina, T.M. Rice, *Phys. Rev. B* 51 (1995) 9253.
- [18] S. Chakravarty, et al., *Phys. Rev. B* 63 (2001) 094503.
- [19] Y. Onose, Y. Taguchi, T. Ishikawa, S. Shinomori, K. Ishizaka, Y. Tokura, *Phys. Rev. Lett.* 82 (1999) 5120.
- [20] I. Bozovic, G. Logvenov, M.A.J. Verhoeven, P. Caputo, E. Goldobin, T.H. Geballe, *Nature* 422 (6934) (2003) 873.